Defining the genes required for survival of *Mycobacterium bovis* in the bovine host offers novel insights into the genetic basis of survival of pathogenic mycobacteria

Amanda J Gibson[1,5&*], Jennifer Stiens[2*], Ian J Passmore[3], Valwynne Faulkner[1,6&], Josephous Miculob[1], Sam Willcocks[3], Michael Coad[4], Stefan Berg[4], Dirk Werling[1], Brendan W Wren[3], Irene Nobeli[2], Bernardo Villarreal-Ramos[4,5&], Sharon L Kendall[1**]

[1]Centre for Emerging, Endemic and Exotic Diseases, Pathobiology and Population Sciences, Royal Veterinary College, Hawkshead Lane, North Mymms, Hatfield, AL9 7TA, United Kingdom.

[2]Institute of Structural and Molecular Biology, Biological Sciences, Birkbeck, University of London, Malet Street, London, WC1E 7HX, United Kingdom.

[3]London School of Hygiene and Tropical Medicine, Keppel Street, London, WC1E 7HT, United Kingdom.

[4]Animal and Plant Health Agency, Woodham Ln, Addlestone, Surrey, KT15 3NB, United Kingdom.

[5]Centre of Excellence for Bovine Tuberculosis, IBERS, Aberystwyth University, Penglais, Aberystwyth, Ceredigion, SY23 3EE, United Kingdom.

[6]Systems Chemical Biology of Infection and Resistance Laboratory, The Francis Crick Institute, 1 Midland Road, London 15 NW1 1AT, United Kingdom.

[&] current address

*the authors contributed equally to the work

**corresponding author

Abstract

Tuberculosis has severe impacts in both humans and animals. Understanding the genetic basis of survival of both *Mycobacterium tuberculosis*, the human adapted species, and *Mycobacterium bovis*, the animal adapted species is crucial to deciphering the biology of both pathogens. There are several studies that identify the genes required for survival of *M. tuberculosis in vivo* using mouse models, however, there are currently no studies probing the genetic basis of survival of *M. bovis in vivo.* In this study we utilise transposon insertion sequencing in *M. bovis* to determine the genes required for survival in cattle. We identify genes encoding established mycobacterial virulence functions such as the ESX-1 secretion system, PDIM synthesis, mycobactin synthesis and cholesterol catabolism that are required *in vivo*. We show that, as in *M. tuberculosis, phoPR* is required by *M. bovis in vivo* despite the known defect in signalling through this system. Comparison to studies performed in glycerol adapted species such as *M. bovis* BCG and *M. tuberculosis* suggests that there are differences in the requirement for genes involved in cholesterol import (*mce4* operon), oxidation (*hsd*) and detoxification (*cyp125*). We report good correlation with existing mycobacterial virulence functions, but also find several novel virulence factors, including genes involved in protein mannosylation, aspartate metabolism and glycerol-phosphate metabolism. These findings further extend our knowledge of the genetic basis of survival *in vivo* in bacteria that cause tuberculosis and provide insight for the development of novel diagnostics and therapeutics.

Importance

This is the first report of the genetic requirements of an animal adapted member of the MTBC in a natural host. *M. bovis* has devastating impacts in cattle and bovine tuberculosis is a considerable economic, animal welfare and public health concern. The data highlight the importance of mycobacterial cholesterol catabolism and identifies several new virulence factors. Additionally, the work informs the development of novel differential diagnostics and therapeutics for TB in both human and animal populations.

Introduction

Bacteria belonging to the *Mycobacterium tuberculosis* complex (MTBC) have devastating impacts in both animal and human populations. *Mycobacterium bovis,* an animal adapted member of the MTBC and one of the main causative agents of bovine tuberculosis (bTB), remains endemic in some high-income settings despite the implementation of a test and slaughter policy. In low- and middle-income settings, the presence of bTB in livestock combined with the absence of rigorous control measures contributes to the risk of zoonotic transmission (1, 2). Control measures based on cattle vaccination utilise the live attenuated vaccine *M. bovis* BCG but the efficacy of this vaccine still remains low in field situations (3, 4). In addition to vaccines, the development of diagnostic tools for the identification of infected individuals is crucial for the management of transmission. Currently, vaccination with *M. bovis* BCG sensitises animals to the diagnostic tuberculin skin test, therefore, sensitive and specific differentiating diagnostic strategies are a current imperative (5, 6).

The increased accessibility of whole genome fitness screens has allowed the assessment of the impacts of the loss of gene function on bacterial survival (7). Such screens have been

72 invaluable in identifying novel drug targets or candidates for the generation of new live
73 attenuated vaccines in a number of bacterial pathogens, including *M. tuberculosis* (8–13).
74 Studies utilising whole genome transposon mutagenesis screens to examine gene fitness *in*
75 *vivo* in *M. tuberculosis* have been limited to mouse models (8, 9, 13). These models do not
76 faithfully replicate the granulomatous pathology associated with TB, nor do mice contain the
77 same repertoire of CD1 molecules expressed by bovine T cells required to present
78 mycobacterial lipid antigens (14). Whole genome transposon mutagenesis screens utilising
79 non-human primates are limited because screening is restricted to smaller mutant pools (15).
80 To date, transposon insertion sequencing (Tn-seq) based studies in the context of bTB in cattle
81 have only been performed using *M. bovis* BCG strains (16, 17).

82 In this study we use Tn-seq to determine the genes required for survival of *M. bovis* directly
83 in cattle. We show that genes involved in the biosynthesis of phthiocerol dimycocerosates
84 (PDIMs), the ESX-1 secretion system, cholesterol catabolism, and mycobactin biosynthesis are
85 essential for survival in cattle, corroborating current knowledge of gene essentiality in
86 members of the MTBC (8, 9, 13, 16, 17). We identify differences in the requirement for genes
87 involved in cholesterol transport and oxidation in the fully virulent *M. bovis* strain. We also
88 identify several novel genes required for survival *in vivo* that have not been previously
89 described in members of the MTBC.

90

91

92

93

Results and Discussion

Generation and sequencing of the input library.

We generated a transposon library in *M. bovis* AF2122/97 using the MycomarT7 phagemid system as previously described (18, 19). Sequencing of the input library showed that transposon insertions were evenly distributed around the genome and 27,751 of the possible 73,536 thymine–adenine dinucleotide (TA) sites contained an insertion representing a saturation density of ~38% (Supplementary Figure S1 and Supplementary Table S1 -input library). The *M. bovis* AF2122/97 genome has 3,989 coding sequences and insertions were obtained in 3,319 of these, therefore the input library contained insertions in 83% of the total coding sequences.

Mycobacterium bovis specific immune responses were observed in cattle

Twenty-four clinically healthy calves of approximately 6 months of age were inoculated with the library through the endobronchial route. Infection was monitored by IFN-γ release assay (IGRA) at the time of inoculation and 2 weeks post infection. *M. bovis* specific immune responses were observed for all study animals at 2 weeks post infection (Figure 1A and B). Each animal presented very low background of circulating IFN-γ together with a statistically significant increase in IFN-γ release in response to PPD-B compared to PPD-A antigens (Figure 1C; *** $p \leq 0.001$). This indicates that infection with the library was successfully established in the cattle.

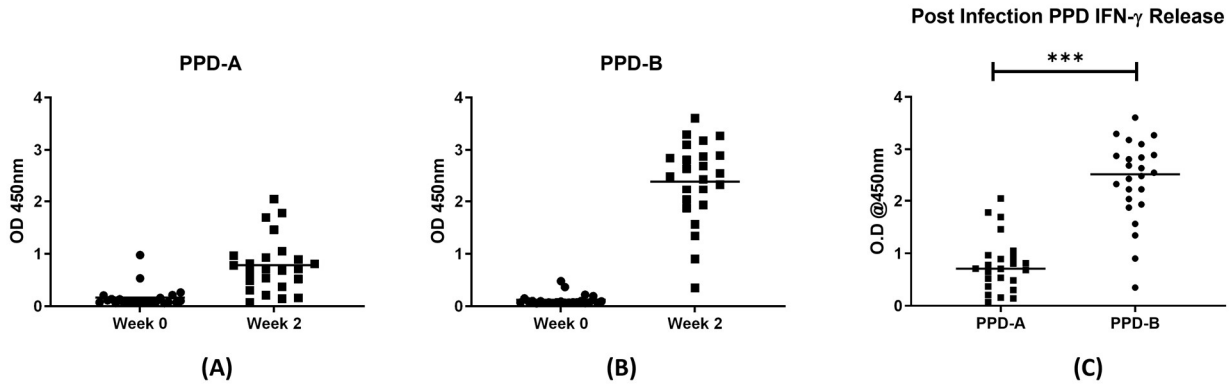

Figure 1. bTB specific IFN-gamma release in cattle infected with the *M. bovis* Tn-library. Blood was collected from all 24 animals on the day of infection and 2 weeks later. No response was detected to either PPD-A or PPD-B antigen stimulation prior to infection (Figure 1A and Figure 1B, week 0). All animals presented a significant and specific response to PPD-B compared to PPD-A as determined by a paired T-test using GraphPad Prism (Figure 1C). *** $p \leq 0.001$

131 **Pathology associated with infection was greater in the lung and thoracic lymph nodes**

132 Animals were culled at 6 weeks post infection. Lung sections and upper (head and neck) and
133 lower (thoracic) respiratory tract associated lymph nodes were examined for gross lesions.
134 Lesions typical of *M. bovis* infection were observed in the tissues examined. Pathology scores
135 are shown in Figure 2A. Greater pathology was observed in lung and thoracic lymph nodes
136 compared to the head and neck lymph nodes.

137

138 **Higher bacterial loads were associated with the lung and thoracic lymph nodes**

139 Bacterial counts were highest in lesions derived from the lung compared to those from the
140 thoracic lymph nodes and head and neck lymph nodes (Figure 2B). The lowest bacterial counts
141 were observed within the head and neck lymph nodes. However, this was not significant when
142 compared to thoracic lymph nodes. The volume of each macerate varied depending on lesion
143 size. Considering macerate volume, average bacterial loads of 10^7, 10^6 and 10^5 were
144 recovered from lesions from samples of the lungs, thoracic lymph nodes and head and neck
145 lymph nodes, respectively.

146

147

148

149

150

151

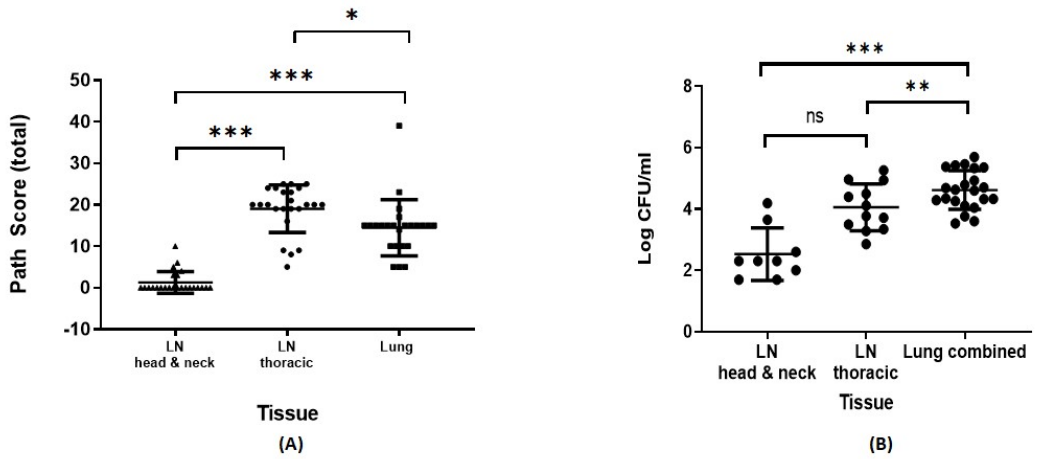

Figure 2. Tissue pathology and bacterial load in tissue sites. Six weeks after infection animals were subjected to post-mortem examination. Gross pathology and evidence of TB-like granulomas lesions were scored. Data presented is the mean across animals of the total scores for each tissue group from 24 animals +/- the standard deviation. Lung and thoracic lymph nodes were observed to contain the highest pathology compared to head and neck lymph nodes (Figure 2A). For bacterial load estimation, aliquots of macerates were plated onto modified 7H11 agar containing kanamycin. Colonies were counted after 3-4 weeks growth. Data are presented as mean CFU/ml per collected tissue group +/- standard deviation. Lung tissue contained the highest bacterial burden compared to thoracic and head and neck lymph nodes as determined by one-way ANOVA analysis using GraphPad Prism (Figure 2b). *** $p \leq 0.001$, ** $p = 0.002$, *$p=0.01$

Recovery and sequencing of *in vivo* selected transposon libraries

In order to recover the Tn library from harvested tissue ~ 10^5-10^6 CFU from lungs and thoracic lymph nodes were plated onto several 140 mm modified 7H11 plates containing kanamycin to minimize competition between mutants. Samples from 4 cattle were lost due to fungal contamination, therefore the samples processed represent samples from 20 cattle. Lung samples were plated from all 20 animals and thoracic lymph nodes samples were plated from 6 cattle. Bacteria were grown for 4-6 weeks before harvesting for genomic DNA extraction and subsequent sequencing (see Supplementary Table S1 for assignation of sequencing files to samples). The diversities of the output libraries were compared to the input library for each sample (Supplementary Figure S2 and Table S1). On average, libraries recovered from lung lesions from 20 different cattle contained 14,456 unique mutants and those recovered from the thoracic lymph nodes contained an average of 16,210 unique mutants. Given that the input library contained 27,751 unique mutants this represented a loss of diversity of ~ 40-50%. Good coverage of coding sequences (CDSs) was maintained as the output libraries still contained insertions in (on average) 68-70% of the open reading frames.

Comparison of the read counts between the input and output libraries allowed a measurement of the impact of the insertion on the survival of mutants in cattle. The results are represented as a mean $\log_2$ fold-change in the output compared with the input for each gene. The entire dataset is shown in supplementary Table S4 and a volcano plot from the lungs and thoracic lymph node of two representative animals is shown in Supplementary Figure S3. Comparison of the mean $\log_2$ fold-change between lung and lymph node samples showed good correlation (Spearman's rho = 0.88, p-value <2.2e-16) (Supplementary Figure S4). TRANSIT resampling was performed to compare the composition of the mutant

194 population in the lungs and thoracic lymph nodes of paired cattle, it was also applied to
195 compare all the thoracic lymph nodes with the lungs of all cattle samples. No statistically
196 significant differences were observed indicating that there were no differences in mutant
197 composition between the tissue sites.

198 No insertion mutants were significantly over-represented in the output library in any of the
199 animals. Although interestingly, insertions in *MB0025,* a gene that is unique to *M. bovis*
200 appeared to improve growth in cattle as mean $\log_2$ fold-changes of +3.9 (lungs) and +4.2
201 (lymph nodes) were observed; however, significance criteria were not met in any of the
202 animals. In order to define a list of attenuating mutations, we used a similar approach to that
203 used in a previous study with an *M. bovis* BCG library in cattle (16). Insertions in genes were
204 defined as attenuating if they had $\log_2$ fold-change of -1.5 or below and an adjusted p-value
205 of <0.05 in at least half of the animals (Table S4, significant in 50% of cattle tab). When using
206 these criteria, there were 141 genes where insertions caused significant attenuation in the
207 lungs or the thoracic lymph nodes, 20 genes that reached significance only in the lungs (shown
208 in red) and 16 genes that reached significance only in the thoracic lymph nodes (shown in
209 green). Of the 141 genes, 109 had been previously described as being required *in vivo* in *M.*
210 *tuberculosis* H37Rv in mouse models through the use of whole genome Tn screens
211 representing ~77% overlap with the previous literature (8, 9, 13).

212

213

214

215

216

Comparison with mutations known to cause attenuation in the MTBC

Insertions in the RD1 encoded ESX-1 type VII secretion system secreting virulence factors and immunodominant antigens EsxA (CFP-10) and EsxB (ESAT-6) are expected to cause attenuation (20). The impacts of insertions in this region are summarised in Figure 3 but are also available in Supplementary Table S4 (RD regions tab) and Supplementary Figure S5. Insertions in genes encoding the structural components of the apparatus (*eccB1, eccCa1, eccCb1, eccD1*) were severely attenuating (log_2 fold-change -6 to -9). Insertions in *eccA1,* which also codes for a structural component of the apparatus, were less impactful (log_2 fold-changes of -2 to -3) despite good insertion saturation in this gene. This is supported by the work of others who have shown that deletion of *eccA1* in *Mycobacterium marinum* leads to only a partial secretion defect (21). There were no impacts seen due to insertions in accessory genes *espJ, espK* and *espH.* The lack of attenuation seen in *espK* mutants is supported by other studies showing that this gene is dispensable for secretion through the apparatus and is not required for virulence of *M. bovis* in guinea pigs (22, 23). Insertions in *esxA* and *esxB* resulted in severe attenuation (log_2 fold-change of -6) but this did not reach significance cut-offs (adj. p=<0.05) in any of the cattle. This is likely to be due to the small number of TAs in these genes which makes it challenging to measure mutant frequency.

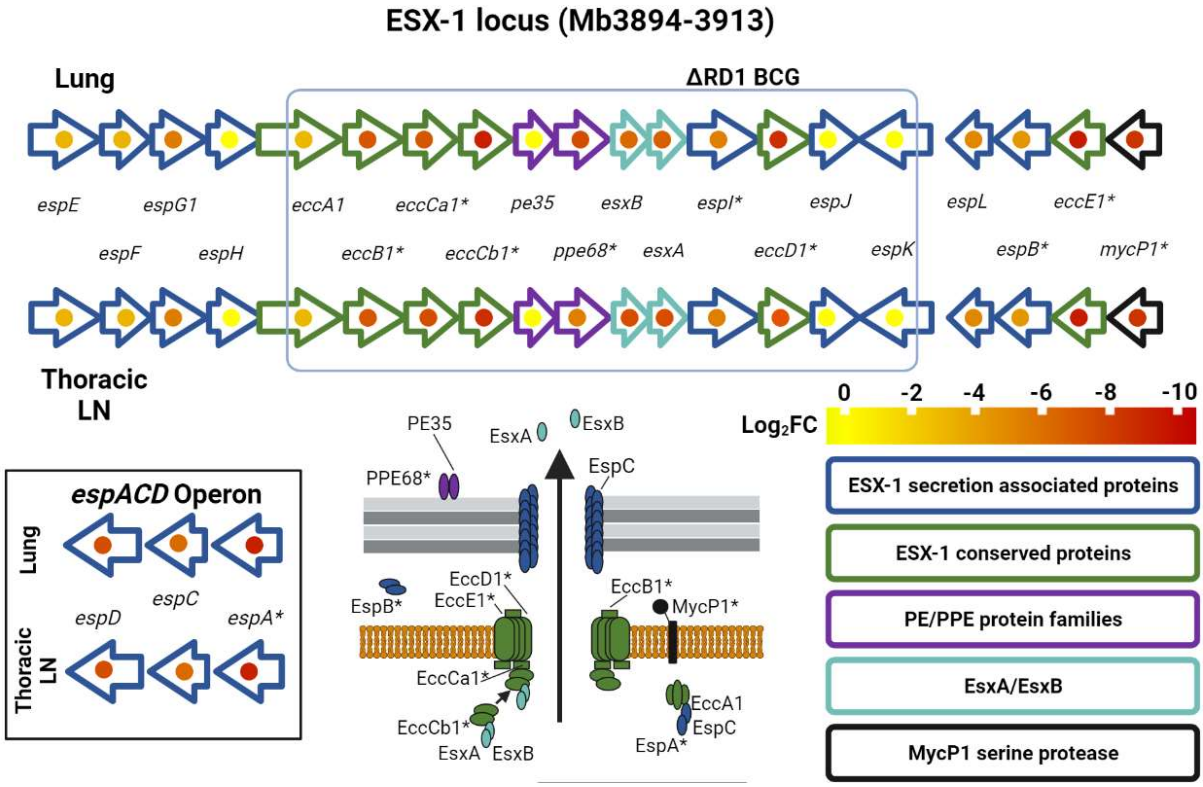

Figure 3. Fold-changes caused by transposon insertions in the ESX-1 secretion system in the lungs and lymph nodes of infected cattle. Asterisks indicate that genes had an adjusted p-value of <0.05 in at least half of the animals. The genes are grouped according to function as indicated by the colour scheme. The $\log_2$ fold-change are indicated on a yellow to red scale and present as a dot in the centre of the gene**.**

The highest levels of attenuation seen were in genes involved in the synthesis of the cell wall virulence lipids PDIMs (*ppsABCDE* and *mas* with $\log_2$ fold-changes of ~-10 commonly seen). PDIM synthesis is well known to be required for the survival of *M. tuberculosis* and *M. bovis* in mice and guinea pigs (24, 25). Insertions in genes involved in the synthesis of PDIMs were the most under-represented ($\log_2$ fold-changes of -8 to -10) in the output library (Figure 4, Supplementary Table S4, mycolipids tab). MmpL7 is involved in PDIM transport and there is evidence that it is phosphorylated by the serine-threonine kinase PknD (26). PknD-MmpL7 interactions are thought to be perturbed in *M. bovis* as *pknD* is split into two coding sequences in the bovine pathogen by a frameshift mutation (27). The data presented here suggest that MmpL7 still functions despite the frameshift mutation.

Iron restriction is thought to be a mechanism by which the host responds to mycobacterial infection, although different cellular compartments may be more restrictive than others (28). Insertion in many of the genes involved in mycobactin synthesis *(Mb2406-Mb2398, mbtJ-mbtH)* were attenuating in cattle (Figure 4, Supplementary Table S4, mycobactin synthesis tab). As mycobactin is required for the acquisition of iron, this confirms that, like other members of the MTBC, needs to scavenge iron from the host for survival (13, 16).

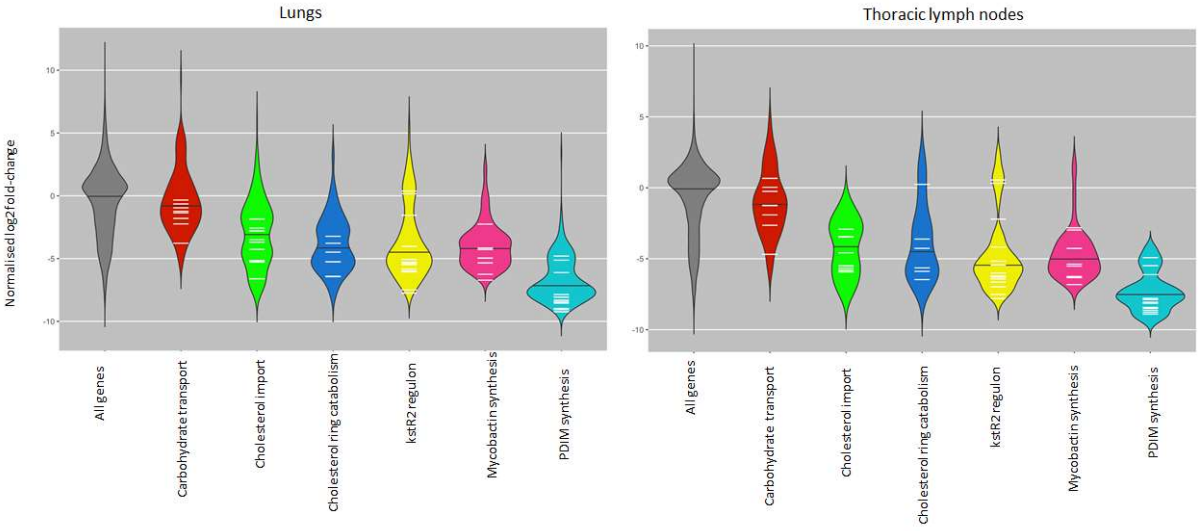

Figure 4. Violin plot of normalised log_2 fold changes in gene insertions recovered from bovine lung or thoracic lymph node tissue samples in selected gene groups. Black bars indicate overall median of normalized log_2 fold-change among genes in grouping. White bars indicate mean log_2 fold-change for each gene in the group across all samples in either lung or lymph node tissue

The role of the cholesterol catabolism in *M. tuberculosis* is well documented and it is required for both energy generation and manipulation of the immune response (29–31). Cholesterol uptake is mediated by the Mce4 transporter coded by the *mce4* operon *Rv3492c-Rv3501c* (*Mb3522c-MB3531c*) (32, 33). It has been suggested that an alternative cholesterol acquisition pathway operates in *M. bovis* BCG Danish as, unlike insertions in genes in the down-stream catabolic pathway, insertions in the *mce4* operon do not result in attenuation in this strain (16). In contrast, our study shows that cholesterol transport via the Mce4 transporter is required in *M. bovis* (Figure 4, Supplementary Table S4 -cholesterol catabolism tab, Figure 5). This corroborates work performed in *M. tuberculosis*, where Mce4 has been shown to be required for growth in chronically infected mice (9, 32). Propionyl-coA generated from the catabolism of cholesterol is toxic and detoxification mechanisms include incorporation into PDIMs (34, 35). The observation that BCG Danish contains a lower amount of PDIMs compared to BCG Pasteur (16) suggests a correlation between Mce4 mediated cholesterol transport and PDIM synthesis and previous studies have demonstrated an increase in PDIM biosynthesis as a result of *mce4* over-expression (36). PDIMs biosynthesis genes are over-expressed in *M. bovis* compared to *M. tuberculosis* (27) and comparison of our dataset with Tn-seq studies performed in *M. tuberculosis* (9) indicates an over-reliance of *M. bovis* on cholesterol transport through the Mce4 transporter (Figure 5).

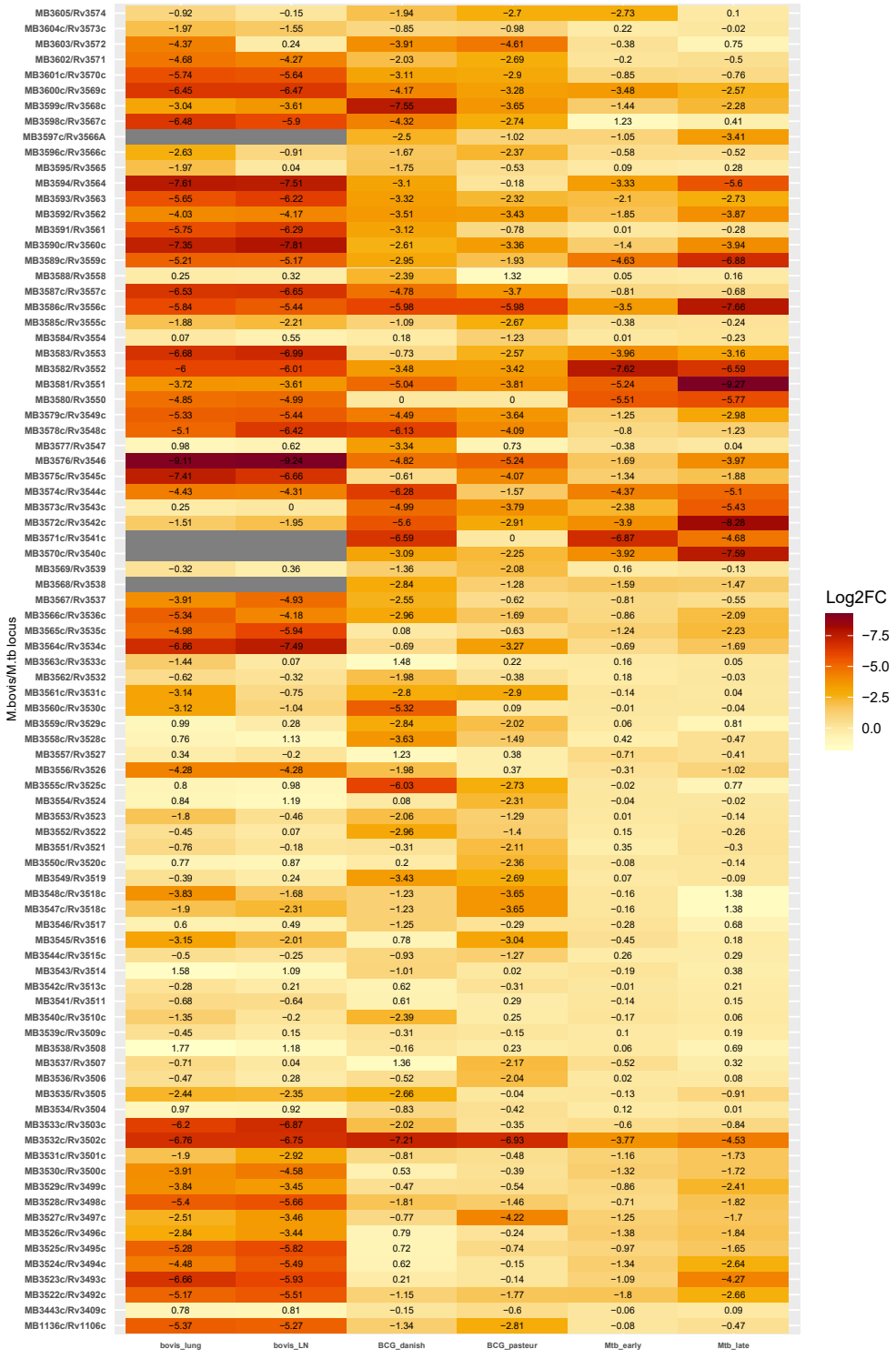

Figure 5. Comparison of reported log_2 fold-change in *M. bovis*, *M. bovis* BCG and Mtb transposon insertion sequencing experiments for orthologous genes in the cholesterol catabolic pathway. Greatest attenuation (most negative log_2 fold-change) is coloured by darkest red. Studies used for comparison include Mendum et al., (24) and Bellarose et al., (9). Grey bars represent genes for which there is no information as they were either ES or GD in input library or had less than 5 insertions in any TA site in any sample (input and all output).

Early stages of cholesterol catabolism involve the oxidation of cholesterol to cholestenone, a reaction catalysed by the 3β-hydroxysteroid dehydrogenase (*hsd*) encoded by *Rv1106c/Mb1136c* (37). The cytochrome P450 Cyp125 (*Mb3575c/Rv3545c*) is required for the subsequent detoxification of cholestenone (38). Insertions in both *hsd* and *cyp125* in *M. bovis* were severely attenuating with $\log_2$ fold-changes of ~-5 to -7 (Supplementary Table S4 - cholesterol catabolism tab, Figure 5). Previous studies have shown that these genes are not required for the survival of *M. tuberculosis* in macrophages or in guinea pigs and this is thought to be due to the availability of other carbon sources, including glycolytic substrates, *in vivo* (37, 39–43). *M. bovis* is more restricted in metabolic capabilities and is unable to generate energy from glycolytic intermediates, largely due to a disrupted pyruvate kinase encoded by *pykA* (44, 45). The essentiality of *hsd* and *cyp125* during infection for *M. bovis* but not *M. tuberculosis* supports the hypothesis of an over-reliance of *M. bovis* on cholesterol. Given the potential for the use of host cholesterol metabolites as diagnostic biomarkers, this observation might have applications in the development of differential diagnostics (46).

Genes that are differentially expressed between *Mycobacterium bovis* and *Mycobacterium tuberculosis*.

Several studies have identified key expression differences between *M. bovis* and *M. tuberculosis* (27, 47, 48). We examined the dataset for insights on the role of differentially expressed genes and transcriptional regulators during infection. One important regulatory system in *M. tuberculosis* is the two-component regulatory system PhoPR and deletions in the *phoPR* genes alongside *fadD26* are attenuating mutations in the live vaccine MTBVAC (49–51). Our data show that insertions in both *phoPR* and *fadD26* were severely attenuating with $\log_2$ fold-changes of -6 to -9 (Figure 6, Supplementary Table S4, *phoPR* regulon tab and

mycolipids tab). This reinforces the role of this system in virulence, despite the presence of a single nucleotide polymorphism (SNP) in the sensor kinase *phoR* that impacts signalling through the system in *M. bovis* (52). Signal potentiation via *phoR* is required for secretion of ESAT-6 through the ESX-1 secretory system and *M. bovis* is known to have compensatory mutations elsewhere in the genome, e.g. in the *espACD* operon, that restores ESAT-6 secretion in the face of a deficient signalling system (49, 52, 53). Our data also show that Tn insertions in *espA* of the *espACD* operon (required for ESAT-6 secretion) and in *mprA*, a transcriptional regulator of that operon (54) were severely attenuating (log2 fold-changes -7 to -9), emphasising the relevance of ESAT-6 as a virulence factor.

Studies comparing differences in expression during *in vitro* growth between *M. bovis* and *M. tuberculosis* show that genes involved in sulfolipid (SL-1) biosynthesis are expressed at lower levels in *M. bovis* compared to *M. tuberculosis* (27, 47). Interestingly, insertions in genes involved in SL-1 biosynthesis (*Mb3850-Mb3856*) are not attenuating *in vivo* (Supplementary File S4, mycolipids tab), reinforcing the lack of importance of SL-1 for *M. bovis in vivo,* at least at the stages of infection studied here.

One of the most highly attenuating insertions occurred in *Mb0222/Rv0216* (log_2 fold change –8 to -9). This gene has been shown to be highly (> 10-fold) over-expressed in *M. bovis* compared with *M. tuberculosis* but the physiological function of this gene is not currently known. The secreted antigens MPB70 and MPB83, encoded by *Mb2900* and *Mb2898* are also over-expressed in *M. bovis* and play a role in host-specific immune responses, however, insertions in these genes did not cause attenuation *in vivo* in our dataset (55).

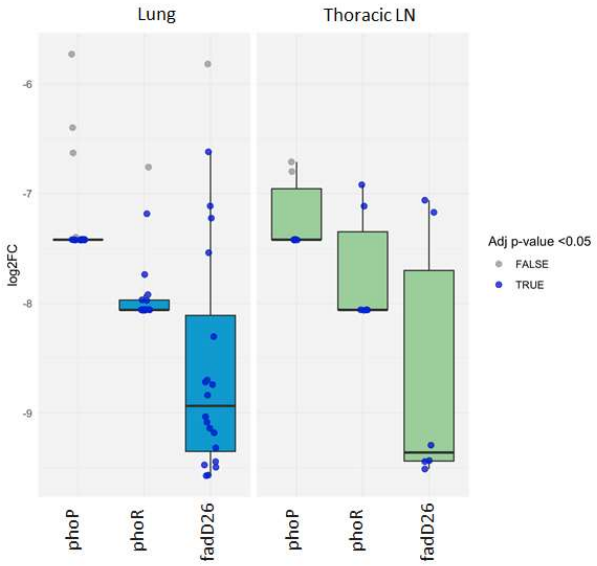

Figure 6. Fold-changes caused by transposon insertions in *phoP, phoR* and *fadD26* in the lungs and lymph nodes of infected cattle. Samples with adjusted p-values (BH-fdr corrected) < 0.05 are indicated with purple points.

Novel attenuating mutations

We identified 32 genes that were required for survival of *M. bovis* in cattle that had not been previously described as being essential *in vivo* through transposon mutagenesis screens of *M. tuberculosis* in mouse models (8, 9, 13) (see Supplementary Table 4, Significant in 50% of cattle tab). While writing this publication, a large scale Tn-seq study that utilised over 120 *M. tuberculosis* libraries and several diverse mouse genotypes (the collaborative cross mouse panel (56)) showed that the panel of genes required for the survival of *M. tuberculosis in vivo* is much larger than previously reported (57). A direct comparison of our dataset with the study by Smith et al., revealed that a further 13 genes were shown to be required in at least one mouse strain in that study. A summary set of the remaining 19 genes is given in Supplementary Table 4, Not in Mtb Tn-seqs tab. Some of these genes have been shown to be attenuated in the mouse model in *M. tuberculosis* through the use of single mutants (58–61).

Included in this list are genes required for phenolic glycolipid synthesis (Figure 7). Insertions in *Mb2971c/Rv2947c* (*pks15/1*) and in *Mb2972c/Rv2948c* (*fadD22*) were attenuating in *M. bovis* but these genes are not required *in vivo* in *M. tuberculosis,* including in the extended panel of mouse genotypes (8, 9, 13, 57). Both *pks15/1* and *fadD22* are involved in the early stages of synthesis of phenolic glycolipids (PGLs) and are involved in virulence (62). The requirement for these genes in *M. bovis* but not in *M. tuberculosis* is consistent with the observation that the Tn-seq studies in *M. tuberculosis* are often carried out using lineage 4 strains (H37Rv and CDC1551) that harbour a frameshift mutation in the *pks15/1* gene, which renders them unable to synthesise PGLs. This removes the requirement for these genes *in*

412 *vivo* in lineage 4 strains of *M. tuberculosis. pks15/1* has been previously reported to be
413 required for survival of *M. bovis* in a guinea pig model of infection (63).

414

415 The list also includes genes that are involved in post-translational modifications such as
416 glycosylation. *Rv1002c* is thought to add mannose groups to secreted proteins and over-
417 expression of this protein in *M. smegmatis* was recently shown to enhance survival *in vivo*
418 and inhibit pro-inflammatory cytokine production (64). The substrates of this protein
419 mannosyltransferase are thought to be several secreted lipoproteins, including LpqW which
420 is involved in the insertion of the virulence lipid LAM at the mycobacterial cell surface (64,
421 65).

422

423

424

425

426

427

428

429

430

431

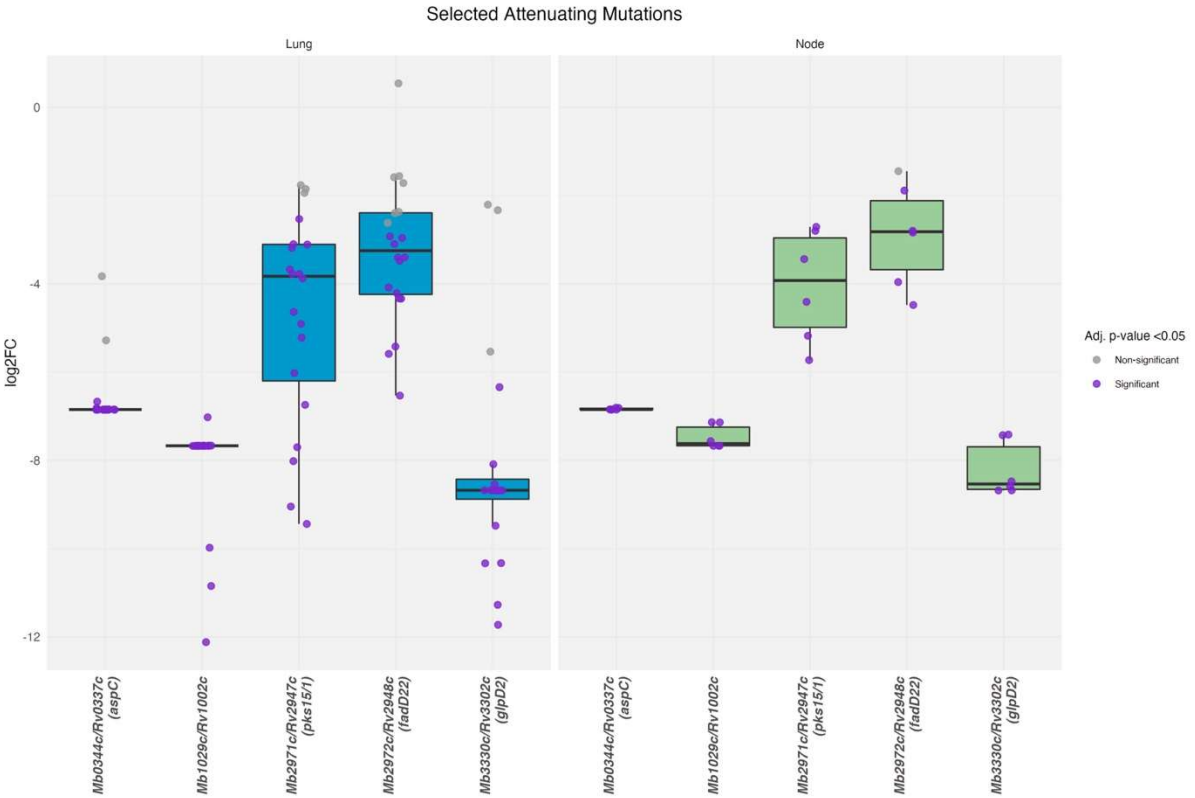

Figure 7. Fold-changes caused by transposon insertions in *pks15/1, fadD22, Rv1002c, aspC* and *glpD2* in the lungs and lymph nodes of infected cattle. Samples with adjusted p-values (BH-fdr corrected) < 0.05 are indicated with purple points.

Finally, this list includes two genes (*aspC* and *glpD2*) that are essential *in vitro* in *M. tuberculosis* but not in *M. bovis* (10, 11, 18, 66). Information regarding *aspC* and *glpD2* from Tn-seq approaches is likely to be lacking in *M. tuberculosis* because Tn mutants will not be represented in the input pool. The absence of insertion mutants in these genes in the most recent large-scale *M. tuberculosis* Tn-seq study supports this (57). One of these genes *MB0344c*/*Rv0337c* (*aspC*) is an aspartate aminotransferase involved in the utilisation of amino acids (aspartate) as a nitrogen source (67). The other gene *Mb3303c*/*Rv3302c* (*glpD2*) is a membrane bound glycerol-phosphate dehydrogenase. In *Escherichia coli*, *glpD2* is an essential enzyme, functioning at the central junction of respiration, glycolysis, and phospholipid biosynthesis and catalyses the oxidation of dihydroxyacetone phosphate (DHAP) from glycerol-3-phosphate resulting in the donation of electrons to the electron transport chain (68). Its essentiality *in vitro* in *M. tuberculosis* might be explained by the usage of glycerol during *in vitro* growth in this species. The contribution of the membrane bound *glpD2* in donation of electrons to the electron transport chain, has been suggested but not yet explored in the MTBC (69). Given the interest in the electron transport chain as a chemotherapeutic target in *M. tuberculosis*, the data presented here suggests that inhibition of *glpD2* might be a fruitful approach in the development of new drugs for the treatment of TB in humans (70). The role of this gene in *M. bovis in vivo* is perhaps surprising, given the disruptions in glycerol phosphate uptake and pathways that phosphorylate glycerol in *M. bovis* AF2122/97 (71). However, *M. tuberculosis* is thought to engage in catabolism of membrane derived glycerophospholipids which may be a potential source of glycerol-3-phosphate in members of the complex (72).

Materials and Methods

Bacterial strains and culture methods

M. bovis strain AF2122/97 was maintained on modified Middlebrook 7H11 (BD Difco™) medium (73). Liquid cultures of *M. bovis* were grown in Middlebrook 7H9 media (BD Difco™) containing 75 mM sodium pyruvate, 0.05% v/v Tween®80 and 10% Middlebrook albumin-dextrose-catalase (ADC) (BBL BD Biosciences). Kanamycin at 25 µg/ml was used for selection where appropriate.

Generation of input transposon mutant library and preparation of the inoculum

Transposon libraries in *M. bovis* were generated as previously described using the MycomarT7 phagemid system as per Majumdar et al with modifications (19). Approximately 66,000 kanamycin resistant transductants were scraped and homogenised in 7H9 medium and stored frozen at -80°C in 1 ml aliquots. CFU counting was performed on the homogenised culture to inform inoculum dosage.

Cattle Infection

Experiments were carried out according to the UK Animal (Scientific Procedures) Act 1986 under project license PPL70/7737. Ethical permission was obtained from the APHA Animal Welfare Ethical Review Body (AWERB) (UK Home Office PCD number 70/6905). All animal infections were carried out within the APHA large animal biocontainment level 3 facility. Twenty-four Holstein-Friesian crosses of 6 months of age were sourced from an officially TB-free herd. An infectious dose of 7 x 10^4 CFU was targeted for the “input” library, allowing

each mutant to be represented in the library ~ 2.5-fold. Retrospective counting of the inoculum revealed the actual inoculum for infection contained 4 x 10^4 CFU. The inoculum was delivered endobronchially in 2 ml of 7H9 medium. In brief, animals were sedated with xylazine (Rompun® 2%, Bayer, France) according to the manufacturer's instructions (0.2 mL/100 kg, IV route) prior to the insertion of an endoscope through the nasal cavity into the trachea for delivery of the inoculum through a 1.8 mm internal diameter cannula (Veterinary Endoscopy Services, U.K.) above the bronchial opening to the cardiac lobe and the main bifurcation between left and right lobes.

Infection Monitoring with the IFN-γ release Assay (IGRA)

Blood was collected by jugular venepuncture from animals on the day of the infectious challenge and two weeks after infection. Heparinized whole blood (250 µl) was incubated with purified protein derivative (PPD) from *M. avium* (PPD-A) or PPD from *M. bovis* (PPD-B) (Prionics™) respectively at 25 IU and 30 IU final. Pokeweed mitogen was used as the positive control at 10 µg/mL and a medium-only negative control. After 24 h incubation in 5% (v/v) CO_2, 95% humidity, 37 °C atmosphere bloods were centrifuged (400 × *g* for 5 min); 120 µl of supernatant was removed and stored at −80 °C for subsequent IFN-γ quantification using the BOVIGAM® kit (Prionics™) in accordance with the manufacturer's instructions.

Collection of tissues and gross pathology scores

Six weeks after the initial infection animals were subjected to post-mortem examination. Initially the experiment was designed with two time points; an early time point (6 weeks) and

a later time point of 8 weeks. However, due to the unexpected high-levels of pathology seen at the earlier time-points all animals were culled at 6 weeks. Gross pathology and evidence of TB-like granulomas lesions was scored using a modified methodology to that previously described in (74). Tissue from head and neck lymph nodes (from the right and left sub-mandibular lymph nodes, the right and left medial retropharyngeal lymph nodes), thoracic lymph nodes (the right and left bronchial lymph nodes, the cranial tracheobronchial lymph nodes, the cranial and caudal mediastinal lymph nodes) and from lung lesions, was collected into sterile containers and frozen at −80 °C until further processing. Frozen tissues were thawed and homogenised in PBS using a Seward Stomacher Paddle Blender.

Recovery of the output transposon mutant library from tissues

Tissue macerates collected from study animals were thawed at room temperature, diluted in PBS and plated on modified 7H11 agar to determine bacterial loads. Colony counts were performed after 3-4 weeks growth. For recovery of the library from tissue macerates ~10^5-10^6 CFU were plated from lung lesions and thoracic lymph node lesions onto modified 7H11 media containing 25 µg/ml kanamycin. The colonies were plated over several 140 mm petri dishes to minimise competition between mutants. The colonies were harvested after 4-6 weeks growth and genomic DNA extracted.

Genomic DNA extraction

Genomic DNA from the input and recovered libraries was isolated by an extended bead beating procedure with detergent-based lysis, phenol-chloroform DNA extraction and

529 precipitation as previously described (18). DNA quality was assessed by nano-spectrometry
530 (DeNovix) and gel electrophoresis and quantified by Qubit analysis using the Broad Range
531 Assay Kit (ThermoScientific).

532

533 **Library preparation for transposon directed insertion sequencing**

534 DNA (2 µg) was resuspended in 50 µL distilled water and sheared to approximately 550 bp
535 fragments using a S220 focussed-ultrasonicator (Covaris), according to the manufacturer's
536 protocol. Fragmented DNA was repaired using NEBNext blunt-end repair kit (New England
537 Biolabs) and purified using Monarch PCR clean-up kit (NEB). Blunted DNA was A-tailed using
538 NEBNext dA-tailing kit (NEB) and column purified. Custom transposon sequencing adaptors
539 (Supplementary Table S3) were generated by heating an equimolar mix of Com_AdaptorPt1
540 primer and Com_AdaptorPt2 (P7+index) primers to 95°C for 5 min, followed by cooling by 1°C
541 every 40 s to a final temperature of 4°C in a thermocycler. Adaptors were ligated to A-tailed
542 library fragments using NEBNext quick ligase kit. Transposon-containing fragments were
543 enriched by PCR using ComP7 primer (10 µM) and an equimolar mix of primers P5-IR2a-d
544 primer (10 µM) in a reaction with 50 ng of adaptor ligated template and Phusion DNA
545 polymerase (NEB) in a thermocycler with the following program 98°C 3 min; 4 cycles of 98°C
546 20s, 70°C 20s, 72°C 1 min; 20 cycles of 98°C 20s, 67°C 20s, 72°C 1 min; 72°C 3 min. Transposon-
547 enriched libraries were subsequently purified with AMPureXP beads (Beckman), pooled
548 together and further purified using AMPure XP beads.

549

550

551 **Data analysis**

552 Indexed libraries were combined, spiked with 20% PhiX, and sequenced on the Illumina Hiseq
553 3000 platform, using v2 chemistry, generating single-end reads of 250 bp. Raw .fastq
554 sequencing files were analysed for quality and pre-processed using the TRANSIT TPP tool (75)
555 set to default 'Sassetti' protocol, in order to remove transposon tags and adapter sequences,
556 and to map reads using BWA-mem to TA sites to the *M. bovis* AF2122/97 genome
557 (NC_002945.3). The TRANSIT 'tnseq_stats' tool was run on each sample to assess insertion
558 density, skew, kurtosis and potential amplification bias.

559 The *M. bovis* AF2122/97 genome was scanned for the non-permissive Himar1 transposon
560 insertion motif ('SGNTANCS', where S is either G or C and N is any base) as previously
561 described [10]. 6605 sites were identified as non-permissive (approximately 9% of total TA
562 sites) and excluded from resampling analysis. A custom annotation, '.prot-table' for TRANSIT,
563 was created from the *M. bovis* AF2122/97 annotation file (NCBI Accession Number LT708304,
564 version LT708304.1). TRANSIT HMM was run on the input library using the default
565 normalisation (TTR) with LOESS correction for genomic position bias. Each TA site was
566 assigned an essentiality state and genes were assigned an essentiality call based on the
567 assigned state of the TA sites within annotated gene boundaries.

568 Resampling between the input library and each of the output sample libraries was performed
569 independently using the TRANSIT resampling algorithm and the complete prot-table. TTR
570 normalisation was used for 23 of the samples, and betageom normalisation for the three
571 samples with skew of greater than 50. The initial resampling output files were evaluated to
572 identify genes with very few, or no, reads at any TA site within the gene boundaries in both
573 the input library and output sample libraries. Genes with no read counts greater than 4 at any

574 TA site, in any sample, and with a sum of all reads at any TA site across the 26 samples less
575 than 55, were flagged. Essential and unchanged genes were removed from the prot-table
576 prior to further evaluation. Resampling was further limited to protein-coding genes.
577 Resampling was re-run for each sample using the attenuated prot-table and an edited
578 TRANSIT resampling script to return the left-tail p-value, as the data were expected to reflect
579 attenuation. All p-values were corrected for multiple testing with FDR adjustment.

580 All analysis and plots were performed using R and R packages, tidyverse and circlize (76–78).
581 Orthologous TB genes were obtained from supplementary data files published by Malone et
582 al, 2018 (27). All scripts, prot-tables and insertion files are available at
583 https://github.com/jenjane118/Mbovis_in-vivo_Tnseq, DOI:10.5281/zenodo.6354151.
584 Sequencing files (.fastq) are deposited in SRA (Bioproject ID: PRJNA816175, Submission ID:
585 SUB11067380)

586

587 **Funding**

588 This work was funded by the BBSRC Grant Ref: BB/N004590/1 [awarded to SK (PI), DW (Co-
589 I), BW (Co-I), and SE3314 to BV-R as part of the joint BBSRC-DEFRA EradbTB consortium. AG,
590 IP, and SW were supported by the funding. VF was in receipt of an RVC PhD studentship. AG
591 currently holds a Sêr Cymru II Lectureship funded by the European Research Development
592 Fund and Welsh Government. BV-R is a Ser Cymru II Professor of Immunology at
593 Aberystwyth University. JS is supported by a Bloomsbury Colleges PhD Studentship (LIDo
594 program).

595

AUTHOR CONTRIBUTIONS

SK, DW, BW, BV-R and SB undertook funding acquisition and designed the study. AJG, VF, JM, SW, IP, MC carried out the experimental work. Data analysis was done by IN and JS. AJG, JS and SLK wrote the first draft of the manuscript. All authors contributed to the manuscript revision, read, and approved the submitted version.

Acknowledgements

The authors would like to acknowledge the help and support of APHA colleagues from the BAC4 workgroup and the Pathology Unit, and in particular acknowledge the care and support provided to animals under experimentation by members of APHA's Animals Sciences Unit. We would like to thank Dr Dany Beste for useful discussions surrounding the role of *glpD2* in mycobacterial metabolism.

608 **References**

609 1. Müller B, Dürr S, Alonso S, Hattendorf J, Laisse CJM, Parsons SDC, van Helden PD,
610 Zinsstag J. 2013. Zoonotic Mycobacterium bovis-induced tuberculosis in humans.
611 Emerg Infect Dis 19:899–908.

612 2. Mableson HE, Okello A, Picozzi K, Welburn SC. 2014. Neglected Zoonotic Diseases—
613 The Long and Winding Road to Advocacy. PLoS Negl Trop Dis 8:e2800.

614 3. Bayissa B, Sirak A, Worku A, Zewude A, Zeleke Y, Chanyalew M, Gumi B, Berg S,
615 Conlan A, Hewinson RG, Wood JLN, Vordermeier HM, Ameni G. 2021. Evaluation of
616 the Efficacy of BCG in Protecting Against Contact Challenge With Bovine Tuberculosis
617 in Holstein-Friesian and Zebu Crossbred Calves in Ethiopia. Front Vet Sci 8.

618 4. Srinivasan S, Conlan AJK, Easterling LA, Herrera C, Dandapat P, Veerasami M, Ameni
619 G, Jindal N, Raj GD, Wood J, Juleff N, Bakker D, Vordermeier M, Kapur V. 2021. A
620 Meta-Analysis of the Effect of Bacillus Calmette-Guérin Vaccination Against Bovine
621 Tuberculosis: Is Perfect the Enemy of Good? Front Vet Sci 0:116.

622 5. Vordermeier HM, Whelan A, Cockle PJ, Farrant L, Palmer N, Hewinson RG. 2001. Use
623 of synthetic peptides derived from the antigens ESAT-6 and CFP-10 for differential
624 diagnosis of bovine tuberculosis in cattle. Clin Diagn Lab Immunol 8:571–578.

625 6. Whelan AO, Clifford D, Upadhyay B, Breadon EL, McNair J, Hewinson GR, Vordermeier
626 MH. 2010. Development of a skin test for bovine tuberculosis for differentiating
627 infected from vaccinated animals. J Clin Microbiol 48:3176–3181.

628 7. Cain AK, Barquist L, Goodman AL, Paulsen IT, Parkhill J, van Opijnen T. 2020. A decade
629 of advances in transposon-insertion sequencing. Nat Rev Genet. Nat Rev Genet.

630 8. Zhang YJ, Reddy MC, Ioerger TR, Rothchild AC, Dartois V, Schuster BM, Trauner A,
631 Wallis D, Galaviz S, Huttenhower C, Sacchettini JC, Behar SM, Rubin EJ. 2013.
632 Tryptophan biosynthesis protects mycobacteria from CD4 T-cell-mediated killing. Cell
633 155:1296–1308.

634 9. Bellerose MM, Proulx MK, Smith CM, Baker RE, Ioerger TR, Sassetti CM. 2020. Distinct
635 Bacterial Pathways Influence the Efficacy of Antibiotics against Mycobacterium
636 tuberculosis. mSystems 5.

637 10. Dejesus MA, Gerrick ER, Xu W, Park SW, Long JE, Boutte CC, Rubin EJ, Schnappinger D,
638 Ehrt S, Fortune SM, Sassetti CM, Ioerger TR. 2017. Comprehensive essentiality
639 analysis of the Mycobacterium tuberculosis genome via saturating transposon
640 mutagenesis. MBio 8.

641 11. Griffin JE, Gawronski JD, Dejesus MA, Ioerger TR, Akerley BJ, Sassetti CM. 2011. High-
642 resolution phenotypic profiling defines genes essential for mycobacterial growth and
643 cholesterol catabolism. PLoS Pathog 7:e1002251.

644 12. Patil S, Palande A, Lodhiya T, Pandit A, Mukherjee R. 2021. Redefining genetic
645 essentiality in Mycobacterium tuberculosis. Gene 765.

646 13. Sassetti CM, Rubin EJ. 2003. Genetic requirements for mycobacterial survival during
647 infection. Proc Natl Acad Sci U S A 100:12989–12994.

648 14. Rhijn I Van, Branch Moody D. CD1 and mycobacterial lipids activate human T cells
649 https://doi.org/10.1111/imr.12253.

650 15. Dutta NK, Mehra S, Didier PJ, Roy CJ, Doyle LA, Alvarez X, Ratterree M, Be NA,
651 Lamichhane G, Jain SK, Lacey MR, Lackner AA, Kaushal D. 2010. Genetic Requirements

for the Survival of Tubercle Bacilli in Primates. J Infect Dis 201:1743–1752.

16. Mendum TA, Chandran A, Williams K, Vordermeier HM, Villarreal-Ramos B, Wu H, Singh A, Smith AA, Butler RE, Prasad A, Bharti N, Banerjee R, Kasibhatla SM, Bhatt A, Stewart GR, McFadden J. 2019. Transposon libraries identify novel Mycobacterium bovis BCG genes involved in the dynamic interactions required for BCG to persist during in vivo passage in cattle. BMC Genomics 20:431.

17. Smith AA, Villarreal-Ramos B, Mendum TA, Williams KJ, Jones GJ, Wu H, McFadden J, Vordermeier HM, Stewart GR. 2020. Genetic screening for the protective antigenic targets of BCG vaccination. Tuberculosis 124:101979.

18. Gibson AJ, Passmore IJ, Faulkner V, Xia D, Nobeli I, Stiens J, Willcocks S, Clark TG, Sobkowiak B, Werling D, Villarreal-Ramos B, Wren BW, Kendall SL. 2021. Probing Differences in Gene Essentiality Between the Human and Animal Adapted Lineages of the Mycobacterium tuberculosis Complex Using TnSeq. Front Vet Sci 8.

19. Majumdar G, Mbau R, Singh V, Warner DF, Dragset MS, Mukherjee R. 2017. Genome-wide transposon mutagenesis in Mycobacterium tuberculosis and Mycobacterium smegmatis, p. 321–335. *In* Methods in Molecular Biology. Humana Press, New York, NY.

20. Lewis KN, Liao R, Guinn KM, Hickey MJ, Smith S, Behr MA, Sherman DR. 2003. Deletion of RD1 from Mycobacterium tuberculosis Mimics Bacille Calmette-Guérin Attenuation . J Infect Dis 187:117–123.

21. Phan TH, van Leeuwen LM, Kuijl C, Ummels R, van Stempvoort G, Rubio-Canalejas A, Piersma SR, Jiménez CR, van der Sar AM, Houben ENG, Bitter W. 2018. EspH is a

hypervirulence factor for Mycobacterium marinum and essential for the secretion of the ESX-1 substrates EspE and EspF. PLoS Pathog 14:e1007247.

22. Inwald J, Jahans K, Hewinson RG, Gordon S V. 2003. Inactivation of the Mycobacterium bovis homologue of the polymorphic RD1 gene Rv3879c (Mb3909c) does not affect virulence. Tuberculosis (Edinb) 83:387–393.

23. Bold TD, Davis DC, Penberthy KK, Cox LM, Ernst JD, de Jong BC. 2012. Impaired fitness of Mycobacterium africanum despite secretion of ESAT-6. J Infect Dis 205:984–90.

24. Hotter GS, Wards BJ, Mouat P, Besra GS, Gomes J, Singh M, Bassett S, Kawakami P, Wheeler PR, De Lisle GW, Collins DM. 2005. Transposon mutagenesis of Mb0100 at the ppe1-nrp locus in Mycobacterium bovis disrupts phthiocerol dimycocerosate (PDIM) and glycosylphenol-PDIM biosynthesis, producing an avirulent strain with vaccine properties at least equal to those of M. bovis BCG. J Bacteriol 187:2267–2277.

25. Cox JS, Chess B, McNeil M, Jacobs WR. 1999. Complex lipid determines tissue-specific replication of Mycobacterium tuberculosis in mice. Nature 402:79–83.

26. Pérez J, Garcia R, Bach H, de Waard JH, Jacobs WR, Av-Gay Y, Bubis J, Takiff HE. 2006. Mycobacterium tuberculosis transporter MmpL7 is a potential substrate for kinase PknD. Biochem Biophys Res Commun 348:6–12.

27. Malone KM, Rue-Albrecht K, Magee DA, Conlon K, Schubert OT, Nalpas NC, Browne JA, Smyth A, Gormley E, Aebersold R, Machugh DE, Gordon S V. 2018. Comparative 'omics analyses differentiate mycobacterium tuberculosis and mycobacterium bovis and reveal distinct macrophage responses to infection with the human and bovine tubercle bacilli. Microb Genomics 4.

696 28. Pisu D, Huang L, Grenier JK, Russell DG. 2020. Dual RNA-Seq of Mtb-Infected
697 Macrophages In Vivo Reveals Ontologically Distinct Host-Pathogen Interactions. Cell
698 Rep 30:335-350.e4.

699 29. Van Der Geize R, Yam K, Heuser T, Wilbrink MH, Hara H, Anderton MC, Sim E,
700 Dijkhuizen L, Davies JE, Mohn WW, Eltis LD. 2007. A gene cluster encoding cholesterol
701 catabolism in a soil actinomycete provides insight into Mycobacterium tuberculosis
702 survival in macrophages. Proc Natl Acad Sci U S A 104:1947–1952.

703 30. Nesbitt NM, Yang X, Fontán P, Kolesnikova I, Smith I, Sampson NS, Dubnau E. 2010. A
704 thiolase of Mycobacterium tuberculosis is required for virulence and production of
705 androstenedione and androstadienedione from cholesterol. Infect Immun 78:275–
706 282.

707 31. Bandyopadhyay U, Chadha A, Gupta P, Tiwari B, Bhattacharyya K, Popli S, Raman R,
708 Brahamachari V, Singh Y, Malhotra P, Natarajan K. 2017. Suppression of Toll-like
709 receptor 2-mediated proinflammatory responses by Mycobacterium tuberculosis
710 protein Rv3529c. J Leukoc Biol 102:1249–1259.

711 32. Pandey AK, Sassetti CM. 2008. Mycobacterial persistence requires the utilization of
712 host cholesterol. Proc Natl Acad Sci U S A 105:4376–4380.

713 33. Mohn WW, Van Der Geize R, Stewart GR, Okamoto S, Liu J, Dijkhuizen L, Eltis LD.
714 2008. The actinobacterial mce4 locus encodes a steroid transporter. J Biol Chem
715 283:35368–35374.

716 34. Lee W, VanderVen BC, Fahey RJ, Russell DG. 2013. Intracellular Mycobacterium
717 tuberculosis exploits host-derived fatty acids to limit metabolic stress. J Biol Chem

718 288:6788–6800.

719 35. Jain M, Petzold CJ, Schelle MW, Leavell MD, Mougous JD, Bertozzi CR, Leary JA, Cox
720 JS. 2007. Lipidomics reveals control of Mycobacterium tuberculosis virulence lipids via
721 metabolic coupling. Proc Natl Acad Sci U S A 104:5133.

722 36. Singh P, Sinha R, Tyagi G, Sharma NK, Saini NK, Chandolia A, Prasad AK, Varma-Basil
723 M, Bose M. 2018. PDIM and SL1 accumulation in Mycobacterium tuberculosis is
724 associated with mce4A expression. Gene 642:178–187.

725 37. Yang X, Gao J, Smith I, Dubnau E, Sampson NS. 2011. Cholesterol Is Not an Essential
726 Source of Nutrition for Mycobacterium tuberculosis during Infection. J Bacteriol
727 193:1473.

728 38. Ouellet H, Guan S, Johnston JB, Chow ED, Kells PM, Burlingame AL, Cox JS, Podust LM,
729 De Montellano PRO. 2010. Mycobacterium tuberculosis CYP125A1, a steroid C27
730 monooxygenase that detoxifies intracellularly generated cholest-4-en-3-one. Mol
731 Microbiol 77:730–742.

732 39. Serafini A, Tan L, Horswell S, Howell S, Greenwood DJ, Hunt DM, Phan MD, Schembri
733 M, Monteleone M, Montague CR, Britton W, Garza-Garcia A, Snijders AP, VanderVen
734 B, Gutierrez MG, West NP, de Carvalho LPS. 2019. Mycobacterium tuberculosis
735 requires glyoxylate shunt and reverse methylcitrate cycle for lactate and pyruvate
736 metabolism. Mol Microbiol 112:1284–1307.

737 40. Safi H, Gopal P, Lingaraju S, Ma S, Levine C, Dartois V, Yee M, Li L, Blanc L, Liang HPH,
738 Husain S, Hoque M, Soteropoulos P, Rustad T, Sherman DR, Dick T, Alland D. 2019.
739 Phase variation in Mycobacterium tuberculosis glpK produces transiently heritable

740 drug tolerance. Proc Natl Acad Sci U S A 116:19665–19674.

741 41. De Carvalho LPS, Fischer SM, Marrero J, Nathan C, Ehrt S, Rhee KY. 2010.
742 Metabolomics of Mycobacterium tuberculosis Reveals Compartmentalized Co-
743 Catabolism of Carbon Substrates. Chem Biol 17:1122–1131.

744 42. Carroll P, Parish T. 2015. Deletion of cyp125 Confers Increased Sensitivity to Azoles in
745 Mycobacterium tuberculosis. PLoS One 10:e0133129.

746 43. Borah K, Mendum TA, Hawkins ND, Ward JL, Beale MH, Larrouy-Maumus G, Bhatt A,
747 Moulin M, Haertlein M, Strohmeier G, Pichler H, Forsyth VT, Noack S, Goulding CW,
748 McFadden J, Beste DJ V. 2021. Metabolic fluxes for nutritional flexibility of
749 Mycobacterium tuberculosis. Mol Syst Biol 17.

750 44. Keating LA, Wheeler PR, Mansoor H, Inwald JK, Dale J, Hewinson RG, Gordon S V.
751 2005. The pyruvate requirement of some members of the Mycobacterium
752 tuberculosis complex is due to an inactive pyruvate kinase: implications for in vivo
753 growth. Mol Microbiol 56:163–174.

754 45. Lofthouse EK, Wheeler PR, Beste DJV, Khatri BL, Wu H, Mendum TA, Kierzek AM,
755 McFadden J. 2013. Systems-based approaches to probing metabolic variation within
756 the Mycobacterium tuberculosis complex. PLoS One 8.

757 46. Chandra P, Coullon H, Agarwal M, Goss CW, Philips JA. 2022. Macrophage global
758 metabolomics identifies cholestenone as host/pathogen cometabolite present in
759 human Mycobacterium tuberculosis infection. J Clin Invest 132.

760 47. Golby P, Hatch KA, Bacon J, Cooney R, Riley P, Allnutt J, Hinds J, Nunez J, Marsh PD,
761 Hewinson RG, Gordon S V. 2007. Comparative transcriptomics reveals key gene

762 expression differences between the human and bovine pathogens of the
763 Mycobacterium tuberculosis complex. Microbiology 153:3323–3336.

764 48. Rehren G, Walters S, Fontan P, Smith I, Zárraga AM. 2007. Differential gene
765 expression between Mycobacterium bovis and Mycobacterium tuberculosis.
766 Tuberculosis (Edinb) 87:347–359.

767 49. Gonzalo-Asensio J, Malaga W, Pawlik A, Astarie-Dequeker C, Passemar C, Moreau F,
768 Laval F, Daffé M, Martin C, Brosch R, Guilhot C. 2014. Evolutionary history of
769 tuberculosis shaped by conserved mutations in the PhoPR virulence regulator. Proc
770 Natl Acad Sci U S A 111:11491–11496.

771 50. White AD, Sibley L, Sarfas C, Morrison A, Gullick J, Clark S, Gleeson F, McIntyre A,
772 Arlehamn CL, Sette A, Salguero FJ, Rayner E, Rodriguez E, Puentes E, Laddy D,
773 Williams A, Dennis M, Martin C, Sharpe S. 2021. MTBVAC vaccination protects rhesus
774 macaques against aerosol challenge with M. tuberculosis and induces immune
775 signatures analogous to those observed in clinical studies. NPJ Vaccines 6.

776 51. Gonzalo-Asensio J, Marinova D, Martin C, Aguilo N. 2017. MTBVAC: Attenuating the
777 Human Pathogen of Tuberculosis (TB) Toward a Promising Vaccine against the TB
778 Epidemic. Front Immunol 8:1803.

779 52. Altes HK, Dijkstra F, Lugnèr A, Cobelens F, Wallinga J. 2009. Targeted bcg vaccination
780 against severe tuberculosis in low-prevalence settings epidemiologic and economic
781 assessment. Epidemiology 20:562–568.

782 53. Frigui W, Bottai D, Majlessi L, Monot M, Josselin E, Brodin P, Garnier T, Gicquel B,
783 Martin C, Leclerc C, Cole ST, Brosch R. 2008. Control of M. tuberculosis ESAT-6

784 secretion and specific T cell recognition by PhoP. PLoS Pathog 4.

785 54. Pang X, Samten B, Cao G, Wang X, Tvinnereim AR, Chen XL, Howard ST. 2013. MprAB
786 regulates the espA operon in Mycobacterium tuberculosis and modulates ESX-1
787 function and host cytokine response. J Bacteriol 195:66–75.

788 55. Queval CJ, Fearns A, Botella L, Smyth A, Schnettger L, Mitermite M, Wooff E,
789 Villarreal-Ramos B, Garcia-Jimenezi W, Heunis T, Trosti M, Werlingi D, Salguero FJ,
790 Gordon S V., Gutierrez MG. 2021. Macrophage-specific responses to human- and
791 animal-adapted tubercle bacilli reveal pathogen and host factors driving
792 multinucleated cell formation. PLoS Pathog 17.

793 56. Churchill GA, Airey DC, Allayee H, Angel JM, Attie AD, Beatty J, Beavis WD, Belknap JK,
794 Bennett B, Berrettini W, Bleich A, Bogue M, Broman KW, Buck KJ, Buckler E,
795 Burmeister M, Chesler EJ, Cheverud JM, Clapcote S, Cook MN, Cox RD, Crabbe JC,
796 Crusio WE, Darvasi A, Deschepper CF, Doerge RW, Farber CR, Forejt J, Gaile D, Garlow
797 SJ, Geiger H, Gershenfeld H, Gordon T, Gu J, Gu W, de Haan G, Hayes NL, Heller C,
798 Himmelbauer H, Hitzemann R, Hunter K, Hsu HC, Iraqi FA, Ivandic B, Jacob HJ, Jansen
799 RC, Jepsen KJ, Johnson DK, Johnson TE, Kempermann G, Kendziorski C, Kotb M, Kooy
800 RF, Llamas B, Lammert F, Lassalle JM, Lowenstein PR, Lu L, Lusis A, Manly KF,
801 Marcucio R, Matthews D, Medrano JF, Miller DR, Mittleman G, Mock BA, Mogil JS,
802 Montagutelli X, Morahan G, Morris DG, Mott R, Nadeau JH, Nagase H, Nowakowski
803 RS, O'Hara BF, Osadchuk A V., Page GP, Paigen B, Paigen K, Palmer AA, Pan HJ,
804 Peltonen-Palotie L, Peirce J, Pomp D, Pravenec M, Prows DR, Qi Z, Reeves RH, Roder J,
805 Rosen GD, Schadt EE, Schalkwyk LC, Seltzer Z, Shimomura K, Shou S, Sillanpää MJ,
806 Siracusa LD, Snoeck HW, Spearow JL, Svenson K, Tarantino LM, Threadgill D, Toth LA,

807 Valdar W, Pardo-Manuel de Villena F, Warden C, Whatley S, Williams RW, Wiltshire T,
808 Yi N, Zhang D, Zhang M, Zou F. 2004. The Collaborative Cross, a community resource
809 for the genetic analysis of complex traits. Nat Genet 2004 3611 36:1133–1137.

810 57. Smith CM, Baker RE, Proulx MK, Mishra BB, Long JE, Park SW, Lee H-N, Kiritsy MC,
811 Bellerose MM, Olive AJ, Murphy KC, Papavinasasundaram K, Boehm FJ, Reames CJ,
812 Meade RK, Hampton BK, Linnertz CL, Shaw GD, Hock P, Bell TA, Ehrt S, Schnappinger
813 D, Pardo-Manuel de Villena F, Ferris MT, Ioerger TR, Sassetti CM. 2022. Host-
814 pathogen genetic interactions underlie tuberculosis susceptibility in genetically
815 diverse mice. Elife 11.

816 58. Cowley S, Ko M, Pick N, Chow R, Downing KJ, Gordhan BG, Betts JC, Mizrahi V, Smith
817 DA, Stokes RW, Av-Gay Y. 2004. The Mycobacterium tuberculosis protein
818 serine/threonine kinase PknG is linked to cellular glutamate/glutamine levels and is
819 important for growth in vivo. Mol Microbiol 52:1691–1702.

820 59. Liu CF, Tonini L, Malaga W, Beau M, Stella A, Bouyssié D, Jackson MC, Nigou J, Puzo G,
821 Guilhot C, Burlet-Schiltz O, Rivière M. 2013. Bacterial protein-O-mannosylating
822 enzyme is crucial for virulence of Mycobacterium tuberculosis. Proc Natl Acad Sci U S
823 A 110:6560–6565.

824 60. Maksymiuk C, Balakrishnan A, Bryk R, Rhee KY, Nathan CF. 2015. E1 of ?-ketoglutarate
825 dehydrogenase defends Mycobacterium tuberculosis against glutamate anaplerosis
826 and nitroxidative stress. Proc Natl Acad Sci U S A 112:E5834–E5843.

827 61. Venugopal A, Bryk R, Shi S, Rhee K, Rath P, Schnappinger D, Ehrt S, Nathan C. 2011.
828 Virulence of Mycobacterium tuberculosis depends on lipoamide dehydrogenase, a

member of three multienzyme complexes. Cell Host Microbe 9:21–31.

62. Constant P, Perez E, Malaga W, Lanéelle MA, Saurel O, Daffé M, Guilhot C. 2002. Role of the pks15/1 Gene in the Biosynthesis of Phenolglycolipids in the Mycobacterium tuberculosisComplex: EVIDENCE THAT ALL STRAINS SYNTHESIZE GLYCOSYLATEDp-HYDROXYBENZOIC METHYL ESTERS AND THAT STRAINS DEVOID OF PHENOLGLYCOLIPIDS HARBOR A FRAMESHIFT MU. J Biol Chem 277:38148–38158.

63. Samanta S, Singh A, Biswas P, Bhatt A, Visweswariah SS. 2017. Mycobacterial phenolic glycolipid synthesis is regulated by cAMP-dependent lysine acylation of FadD22. Microbiol (United Kingdom) 163:373–382.

64. Yang S, Sui S, Qin Y, Chen H, Sha S, Liu X, Deng G, Ma Y. 2022. Protein O-mannosyltransferase Rv1002c contributes to low cell permeability, biofilm formation in vitro, and mycobacterial survival in mice. APMIS 130:181–192.

65. Crellin PK, Kovacevic S, Martin KL, Brammananth R, Morita YS, Billman-Jacobe H, McConville MJ, Coppel RL. 2008. Mutations in pimE restore lipoarabinomannan synthesis and growth in a Mycobacterium smegmatis lpqW mutant. J Bacteriol 190:3690–3699.

66. Butler RE, Smith AA, Mendum TA, Chandran A, Wu H, Lefrançois L, Chambers M, Soldati T, Stewart GR. 2020. Mycobacterium bovis uses the ESX-1 Type VII secretion system to escape predation by the soil-dwelling amoeba Dictyostelium discoideum. ISME J 14:919.

67. Agapova A, Serafini A, Petridis M, Hunt DM, Garza-Garcia A, Sohaskey CD, de Carvalho LPS. 2019. Flexible nitrogen utilisation by the metabolic generalist pathogen

Mycobacterium tuberculosis. Elife 8.

68. Yeh JI, Chinte U, Du S. 2008. Structure of glycerol-3-phosphate dehydrogenase, an essential monotopic membrane enzyme involved in respiration and metabolism. Proc Natl Acad Sci U S A 105:3280.

69. Cook GM, Hards K, Dunn E, Heikal A, Nakatani Y, Greening C, Crick DC, Fontes FL, Pethe K, Hasenoehrl E, Berney M. 2017. Drug Discovery & Development: State-of-the-Art and Future Directions" on the topic of "Targets": OXPHOS as a target space for tuberculosis: success, caution, and future directions. Microbiol Spectr 5.

70. Bald D, Villellas C, Lu P, Koul A. 2017. Targeting energy metabolism in Mycobacterium tuberculosis, a new paradigm in antimycobacterial drug discovery. MBio 8.

71. Garnier T, Eiglmeier K, Camus J-C, Medina N, Mansoor H, Pryor M, Duthoy S, Grondin S, Lacroix C, Monsempe C, Simon S, Harris B, Atkin R, Doggett J, Mayes R, Keating L, Wheeler PR, Parkhill J, Barrell BG, Cole ST, Gordon S V., Hewinson RG. 2003. The complete genome sequence of Mycobacterium bovis. Proc Natl Acad Sci U S A 100:7877.

72. Larrouy-Maumus G, Biswas T, Hunt DM, Kelly G, Tsodikov O V., De Carvalho LPS. 2013. Discovery of a glycerol 3-phosphate phosphatase reveals glycerophospholipid polar head recycling in Mycobacterium tuberculosis. Proc Natl Acad Sci U S A 110:11320–11325.

73. Gallagher J, Horwill DM. 1977. A selective oleic acid albumin agar medium for the cultivation of Mycobacterium bovis. J Hyg (Lond) 79:155.

74. Vordermeier HM, Chambers MA, Cockle PJ, Whelan AO, Simmons J, Hewinson RG.

873 2002. Correlation of ESAT-6-specific gamma interferon production with pathology in
874 cattle following Mycobacterium bovis BCG vaccination against experimental bovine
875 tuberculosis. Infect Immun 70:3026–3032.

876 75. DeJesus MA, Ambadipudi C, Baker R, Sassetti C, Ioerger TR. 2015. TRANSIT--A
877 Software Tool for Himar1 TnSeq Analysis. PLoS Comput Biol 11.

878 76. Gu Z, Gu L, Eils R, Schlesner M, Brors B. 2014. circlize Implements and enhances
879 circular visualization in R. Bioinformatics 30:2811–2812.

880 77. R Core Team. R: A Language and Environment for Statistical Computing.

881 78. Wickham H, Averick M, Bryan J, Chang W, D' L, Mcgowan A, François R, Grolemund G,
882 Hayes A, Henry L, Hester J, Kuhn M, Lin Pedersen T, Miller E, Bache SM, Müller K,
883 Ooms J, Robinson D, Seidel DP, Spinu V, Takahashi K, Vaughan D, Wilke C, Woo K,
884 Yutani H. 2019. Welcome to the Tidyverse. J Open Source Softw 4:1686.

885

886

887 **Figure Legends**

888 **Figure 1. bTB specific IFN-gamma release in cattle infected with the *M. bovis* Tn-library.**
889 Blood was collected from all 24 animals on the day of infection and 2 weeks later. No response
890 was detected to either PPD-A or PPD-B antigen stimulation prior to infection (Figure 1A and
891 Figure 1B, week 0). All animals presented a significant and specific response to PPD-B
892 compared to PPD-A as determined by a paired T-test using GraphPad Prism (Figure 1C). ***
893 $p \leq 0.001$

894

895 **Figure 2. Tissue pathology and bacterial load in tissue sites. Six weeks after infection**
896 **animals were subjected to post-mortem examination.** Gross pathology and evidence of TB-
897 like granulomas lesions were scored. Data presented is the mean across animals of the total
898 scores for each tissue group from 24 animals +/- the standard deviation. Lung and thoracic
899 lymph nodes were observed to contain the highest pathology compared to head and neck
900 lymph nodes (Figure 2A). For bacterial load estimation, aliquots of macerates were plated
901 onto modified 7H11 agar containing kanamycin. Colonies were counted after 3-4 weeks
902 growth. Data are presented as mean CFU/ml per collected tissue group +/- standard
903 deviation. Lung tissue contained the highest bacterial burden compared to thoracic and head
904 and neck lymph nodes as determined by one-way ANOVA analysis using GraphPad Prism
905 (Figure 2b). *** $p \leq 0.001$, ** $p = 0.002$, *$p=0.01$

906

907 **Figure 3. Fold-changes caused by transposon insertions in the ESX-1 secretion system in the**
908 **lungs and lymph nodes of infected cattle.** Asterisks indicate that genes had an adjusted p-

909 value of <0.05 in at least half of the animals. The genes are grouped according to function as
910 indicated by the colour scheme. The log_2 fold-change are indicated on a yellow to red scale
911 and present as a dot in the centre of the gene**.**

912

913 **Figure 4. Violin plot of normalised log_2 fold changes in gene insertions recovered from**
914 **bovine lung or thoracic lymph node tissue samples in selected gene groups.** Black bars
915 indicate overall median of normalized log_2 fold-change among genes in grouping. White bars
916 indicate mean log_2 fold-change for each gene in the group across all samples in either lung or
917 lymph node tissue

918

919 **Figure 5. Comparison of reported log_2 fold-change in *M. bovis*, *M. bovis* BCG and Mtb**
920 **transposon insertion sequencing experiments for orthologous genes in the cholesterol**
921 **catabolic pathway.** Greatest attenuation (most negative log_2 fold-change) is coloured by
922 darkest red. Studies used for comparison include Mendum et al., (24) and Bellarose et al., (9).
923 Grey bars represent genes for which there is no information as they were either ES or GD in
924 input library or had less than 5 insertions in any TA site in any sample (input and all output).

925

926 **Figure 6. Fold-changes caused by transposon insertions in *phoP, phoR* and *fadD26* in the**
927 **lungs and lymph nodes of infected cattle.** Samples with adjusted p-values (BH-fdr corrected)
928 < 0.05 are indicated with purple points.

929